Acta Pharmacologica Sinica 2017: 1663–1672
 1671-4083/17
www.nature.com/aps

Original Article

Functional expression of the Ca^{2+} signaling machinery in human embryonic stem cells

Ji-jun HUANG[1, 2, #], Yi-jie WANG[2, #], Min ZHANG[2, #], Peng ZHANG[2], He LIANG[2], Hua-jun BAI[2], Xiu-jian YU[2], Huang-tian YANG[1, 2, 3, *]

[1]Heart Center, Shanghai Jiao Tong University Affiliated Sixth People's Hospital, Shanghai 200233, China; [2]Key Laboratory of Stem Cell Biology, Institute of Health Sciences, Shanghai Institutes for Biological Sciences, Chinese Academy of Sciences & Shanghai Jiao Tong University School of Medicine, Shanghai 200031, China; [3]Second Affiliated Hospital, Zhejiang University, Hangzhou 310009, China

Abstract

Emerging evidence suggests that Ca^{2+} signals are important for the self-renewal and differentiation of human embryonic stem cells (hESCs). However, little is known about the physiological and pharmacological properties of the Ca^{2+}-handling machinery in hESCs. In this study we used RT-PCR and Western blotting to analyze the expression profiles of genes encoding Ca^{2+}-handling proteins; we also used confocal Ca^{2+} imaging and pharmacological approaches to determine the contribution of the Ca^{2+}-handling machinery to the regulation of Ca^{2+} signaling in hESCs. We revealed that hESCs expressed pluripotent markers and various Ca^{2+}-handling-related genes. ATP-induced Ca^{2+} transients in almost all hESCs were inhibited by the inositol-1,4,5-triphosphate receptor (IP_3R) blocker 2-APB or xestospongin C. In addition, Ca^{2+} transients were induced by a ryanodine receptor (RyR) activator, caffeine, in 10%–15% of hESCs and were blocked by ryanodine, whereas caffeine and ATP did not have additive effects. Moreover, store-operated Ca^{2+} entry (SOCE) but not voltage-operated Ca^{2+} channel-mediated Ca^{2+} entry was observed. Inhibition of sarco/endoplasmic reticulum (ER) Ca^{2+}-ATPase (SERCA) by thapsigargin induced a significant increase in the cytosolic free Ca^{2+} concentration ($[Ca^{2+}]_i$). For the Ca^{2+} extrusion pathway, inhibition of plasma membrane Ca^{2+} pumps (PMCAs) by carboxyeosin induced a slow increase in $[Ca^{2+}]_i$, whereas the Na^+/Ca^{2+} exchanger (NCX) inhibitor KBR7943 induced a rapid increase in $[Ca^{2+}]_i$. Taken together, increased $[Ca^{2+}]_i$ is mainly mediated by Ca^{2+} release from intracellular stores via IP_3Rs. In addition, RyRs function in a portion of hESCs, thus indicating heterogeneity of the Ca^{2+}-signaling machinery in hESCs; maintenance of low $[Ca^{2+}]_i$ is mediated by uptake of cytosolic Ca^{2+} into the ER via SERCA and extrusion of Ca^{2+} out of cells via NCX and PMCA in hESCs.

Keywords: Ca^{2+} signaling; Ca^{2+} release; Ca^{2+} extrusion; Ca^{2+} channels; Ca^{2+} pumps; human embryonic stem cells

Acta Pharmacologica Sinica (2017) 38: 1663–1672; doi: 10.1038/aps.2017.29; published online 17 Jul 2017

Introduction

Human embryonic stem cells (hESCs) are derived from the inner cell mass of human embryos and have the potential to differentiate into all cell types of the body. They have been widely studied as models of early development, in drug screening and as potential candidates in cell therapy in recent years[1–4]. Emerging evidence suggests that the calcium ion (Ca^{2+}) is an important second messenger involved in the maintenance of the pluripotency and self-renewal of hESCs and takes part in the differentiation of these cells[5–9]. However, little is known about the physiological and pharmacological properties of Ca^{2+} signaling and how the intracellular free Ca^{2+} concentration ($[Ca^{2+}]_i$) is regulated in hESCs.

Current knowledge of the Ca^{2+}-handling mechanisms in pluripotent stem cells is mainly from the study of mouse embryonic stem cells (mESCs)[10, 11]. The increased $[Ca^{2+}]_i$ in mESCs is mainly mediated by Ca^{2+} entry through store-operated Ca^{2+} entry (SOCE) via store-operated Ca^{2+} channels (SOCCs)[10], and the Ca^{2+} is released from internal stores via inositol triphosphate receptors (IP_3Rs) but not ryanodine receptors (RyRs). Accordingly, the decrease in $[Ca^{2+}]_i$ is mediated by pumping cytosolic Ca^{2+} back into the endoplasmic reticulum (ER) via sarco/endoplasmic reticulum Ca^{2+}-ATPase (SERCA) and extrusion of Ca^{2+} from the cell by the Na^+/Ca^{2+} exchanger (NCX) and plasma membrane Ca^{2+} ATPase (PMCA) in mESCs[10]. However, whether hESCs share similar Ca^{2+}-handling mechanism with mESCs is unclear. Recently, we and others have found that Ca^{2+} signals are triggered by purinergic stimulation in hESCs[5, 7, 9]. We further demonstrated that this

[#] These authors contributed equally to this work.
[*] To whom correspondence should be addressed.
E-mail htyang@sibs.ac.cn
Received 2016-11-24 Accepted 2017-03-13

effect is mediated via the purinergic receptor P2Y1-IP_3R2 pathway[5]. However, the properties of the Ca^{2+}-handling machinery in hESCs are largely unknown. In addition, spontaneous Ca^{2+} activity is observed in mESCs[12], but whether this event occurs in hESCs remains to be elucidated.

In this study, we sought to illustrate the physiological and pharmacological properties of the Ca^{2+}-handling machinery in the plasma and internal stores of hESCs through gene expression analysis and confocal Ca^{2+} imaging combined with pharmacological approaches. Our findings provide new insight into the functional regulatory pathways of Ca^{2+} signaling in hESCs.

Materials and methods

hESC culture

hESC culture was carried out as described previously[5, 13]. Briefly, hESC lines H7 and H9 (WiCell Research Institute, Madison, WI, USA) were routinely maintained in mTeSR1 medium (Stem Cell Technologies, Vancouver, Canada) on Matrigel-coated dishes (hESC qualified; Corning, New York, NY, USA). For Ca^{2+} imaging, hESCs were digested to single cells by Accutase and were seeded onto Matrigel-coated 20-mm glass-bottom dishes (Nest Scientific, Rahway, NJ, USA) at a density of 3.5×10^4 cells/cm^2 in mTeSR1. The medium was changed every day. Then, 36–48 h after seeding, hESC clones were used for Ca^{2+} imaging to allow for homogenous loading of the Ca^{2+} indicator. To decrease apoptosis, 5 mmol/L Rho-associated, coiled-coil containing protein kinase inhibitor Y27632 (Stem Cell Technologies, Vancouver, Canada) was added for the first 24 h after cell seeding.

Ca^{2+} imaging

hESCs were loaded with 2.5 μmol/L Fluo4-AM (Life Technologies, South San Francisco, CA, USA) as reported previously[5]. Briefly, the Fluo 4-AM was dissolved in the extracellular bath solution for 30 min at 37 °C. Then, the Ca^{2+} indicator was washed out three times with the bath solution, and the cells were used 30 min later at room temperature for the de-esterification of the dye. The fluorescence of hESCs was measured with a confocal laser scanning microscope (LSM 710, Carl Zeiss, Oberkochen, Germany) with a 20× objective. The fluorescence was excited with a wavelength of 488 nm, and the emission light was collected with a wavelength >493 nm. Images were acquired every 2 s.

Immunostaining

Immunostaining assays were performed as previously described[5]. Briefly, the cells were fixed with 4% paraformaldehyde, permeabilized in 0.3% Triton X-100 for the detection of intracellular antigens (Sigma, Saint Louis, MO, USA), blocked in 10% normal goat serum (Vector Laboratories, Burlingame, CA, USA), and then incubated with primary antibodies against OCT4 (1:400; Abcam, Cambridge, UK) or NANOG (1:100; Abcam, Cambridge, UK) at 4 °C overnight, and the primary antibodies were detected with DyLight 488- or 549-conjugated secondary antibodies (Jackson ImmunoResearch Laboratories, West Grove, PA, USA). Nuclei were stained with DAPI (Sigma, Saint Louis, MO, USA). A Zeiss Observer microscope was used for slide observation and image capture.

Flow cytometry analysis

Cells were harvested and dissociated with Accutase (Stem Cell Technologies, Vancouver, Canada). Samples were blocked with 3% fetal bovine serum and were then stained for the presence of appropriate hESCs markers by using FITC-conjugated SSEA4 antibody (1:100; BD Biosciences, San Jose, CA, USA) or isotype-matched negative controls.

Analysis of Ca^{2+} responses

The analysis of Ca^{2+} responses was based on the customer-modified Interactive Data Language (IDL, ITT corporation, White Plains, NY, USA) Program, Flash Sniper as reported previously[5, 14]. Briefly, the images recorded were opened in Flash Sniper, and a mask was set up to exclude the noise signals from non-cell regions. The regions of interest (ROIs) were manually selected for each cell. The normalized amplitude of a Ca^{2+} transient was expressed as $dF/F_0=(F_1-F_0)/F_0$, where F_0 and F_1 are the values of the fluorescence intensity at rest and the peak time point, respectively. For each ROI, the start time and end time of Ca^{2+} transients were set manually, and dF/F_0 was calculated with Flash Sniper. Finally, traces representing the fluorescence intensity changes were automatically generated by the software. The cells with $dF/F_0>0.2$ were defined as responding cells. For the calculation of the amplitude values, at least more than 30 responding cells were randomly selected from each field, whereas all of the responding cells were chosen when the total responding cell number was <30 in the experiment. All of the cells in each imaging field were counted to calculate the responding percentage. The responding cell percentage was calculated as the responding cell number/total cell number examined. At least three independent experiments were performed for each of the reagents.

Reverse transcription (RT)-PCR

Total RNA was prepared using an RNeasy Plus Mini Kit (QIAGEN, Hilden, Germany) according to the manufacturer's instructions and treated with RNase-Free DNAse (Promega, Madison, WI, USA) for 15 min to eliminate the potential contamination of genomic DNA. cDNAs were generated through reverse transcription of total RNA (1 μg) with ReverTra Ace reverse transcriptase (Toyobo, Osaka, Japan). The RT-PCR was carried out using 2× Taq Plus Master Mix (Vazyme, Piscataway, NJ, USA). GAPDH was used as the endogenous control, and samples that did not undergo reverse transcription were used as negative controls. The RT-PCR primers were self-designed or selected from the Primer Bank and are listed in Supporting Information Table S1.

Western blot analysis

hESCs and 293FT cells were harvested by scraping, and total proteins were extracted with lysis buffer (40 mmol/L Tris, 150 mmol/L NaCl, 1 mmol/L EDTA, 1% Triton X-100, 0.1% SDS, and protease inhibitor cocktail added before use). The protein

(100 μg for each sample) was separated by 8% SDS-PAGE and transferred onto a nitrocellulose membrane. Membranes were blocked in 0.1% Tween 20-TBS with 3% BSA. Primary antibodies were incubated overnight at 4 °C, and secondary antibodies were incubated for 1 h at room temperature, and membranes were washed with TBST 3 times before imaging. Membranes were scanned using an Odyssey CLx (LI-COR). The primary antibodies were anti-Cav1.2 (1:500, Santa Cruz, sc-398433), anti-Cav1.3 (1:500, Abcam, ab85491), anti-Cav1.4 (1:500, Abcam, ab171968), anti-Cav3.1 (1:500, Abcam, ab209526), and anti-Cav3.2 (1:500, Abcam, ab135974).

Reagents and solutions

Carboxyeosin was purchased from Molecular Probes (Eugene, OR, USA). 2-[2-[4-(4-nitrobenzyloxy) phenyl]ethyl] isothiourea methanesulfonate (KB-R7943) and thapsigargin were purchased from Tocris Biosciences Ltd (Bristol, UK). All of the other reagents were purchased from Sigma (Saint Louis, MO, USA). Reagents were directly dissolved in distilled water except for carboxyeosin, thapsigargin, KB-R7943 and 2-aminoethoxydiphenyl borate (2-APB), which were dissolved in 0.1% DMSO. The standard extracellular bath solution contained (in mmol/L) NaCl, 135; KCl, 5.4; $CaCl_2$, 1.8; $MgCl_2$, 1.0; glucose, 10; and HEPES, 10 (pH adjusted to 7.4). For the Ca^{2+}-free solution, extracellular $CaCl_2$ was removed, and 1 mmol/L EGTA was added. For the high Ca^{2+} concentration solution, 4 mmol/L Ca^{2+} was used instead of 1.8 mmol/L Ca^{2+} in the standard extracellular bath solution. For the high K^+ concentration solution, 145 mmol/L K^+ was used instead of 135 mmol/L Na^+ and 5.4 mmol/L K^+ in the standard extracellular bath solution.

Statistical analysis

The data are presented as the means±SEM. A Two-way ANOVA with Bonferroni post-test was used for analyzing caffeine-induced dF/F_0 or the percentage of responding cells compared with that induced by ATP (Figure 3A) or in control *vs* Ca^{2+}-free conditions (Figure 3B). A one-way ANOVA with Bonferroni post-test was used in Figure 3F and 3G. A two-tailed *t*-test was used to analyze the data in Figure S1B, Figure 5B, 5C and 5D–5F. All statistical analyses were performed by using GraphPad Prism 5 (San Diego, CA, USA). $P<0.05$ was considered statistically significant.

Results

Spontaneous and ATP-induced Ca^{2+} activity in hESCs

To determine the Ca^{2+} signaling properties of hESCs, we first examined the pluripotent characteristics of H9 and H7 hESCs used in this study. Immunostaining analysis showed that hESCs homogenously expressed pluripotent markers OCT4 and NANOG, and flow cytometry analysis further confirmed the high expression of the pluripotent marker SSEA4 (Supplementary Figure 1A and 1B), thus indicating the undifferentiated state of hESCs. Next, we analyzed the spontaneous Ca^{2+} activity in steady states of hESCs by using a confocal Ca^{2+} imaging system. No spontaneous Ca^{2+} activity in individual cells of hESC clones was detected by confocal imaging during a 600-s examination period in H9 (Figure 1A, left) and H7 hESCs (Figure 1A, right). This phenomenon was further confirmed in recordings up to 20 min (data not show). In contrast, extracellular ATP at 100 μmol/L induced a rapid Ca^{2+} transient in both H9 (Figure 1B, left) and H7 hESCs (Figure 1B, right) as we have reported previously[5], and the enhanced $[Ca^{2+}]_i$ quickly declined to basal levels even in the presence of ATP (Figure 1B). To determine whether IP_3Rs, the main Ca^{2+}-release channels located on the intercellular Ca^{2+} stores[15], contribute to the ATP-induced increase in $[Ca^{2+}]_i$, two IP_3R blockers, 2-APB (100 μmol/L)[10] and xestospongin C (20 μmol/L)[16] (Figure 1C, lower panels) were added before ATP. 2-APB and xestospongin C (Figure 1C) completely inhibited the ATP-induced Ca^{2+} transients in hESCs, whereas vehicle DMSO (0.1%) did not have any effect on $[Ca^{2+}]_i$ in these cells (Supplementary Figure 2). These results indicated that hESCs, at least H7 and H9 cells, do not have active spontaneous Ca^{2+} activity in the steady state but have Ca^{2+} responses to extracellular ATP via Ca^{2+} release from IP_3Rs.

Expression profiles of Ca^{2+}-handling genes in hESCs

We then hypothesized that the Ca^{2+} signaling regulatory machinery responsible for Ca^{2+} homeostasis exists in hESCs. To test this hypothesis, we analyzed the expression of genes encoding the main Ca^{2+}-handling channels or pumps in hESCs. For the ER Ca^{2+}-release channels, in addition to the expression of *ITPR1-3* genes (coding IP_3R1-3) that was previously detected in hESCs (Figure 2A)[5], surprisingly, the expression of *RyR1-3* was detected in hESCs (Figure 2A), which has been reported to be absent in non-excitable cells[17]. To determine the molecular basis for Ca^{2+} entry, we screened all members of T-type and L-type Ca^{2+} channels, which belong to the voltage-operated Ca^{2+} channels (VOCCs[18, 19]). Among three subtypes of T-type Ca^{2+} channels, the *Cav3.1* and *Cav3.2* expression was dominant, whereas *Cav3.3* was scarcely detected in hESCs; among four subtypes of L-type Ca^{2+} channels, *Cav1.2*, *Cav1.3* and *Cav1.4* but not *Cav1.1* were detected in hESCs (Figure 2B). Because Ca^{2+} release-activated calcium modulators (ORAIs) and transient receptor potential cation channels (TRPCs) are two types of SOCCs responsible for Ca^{2+} influx into cells[20, 21], we screened all subtypes of both channels. All ORAI members (*ORAI1-3*) were detected in hESCs (Figure 2C), whereas *TRPC3, 4a, 4e, 5, 6,* and *7* but not *TRPC1* were detected in these cells (Figure 2C). For the genes encoding Ca^{2+}-handling proteins responsible for the decrease in $[Ca^{2+}]_i$, the expression of *SERCA2-3* for the ER Ca^{2+}-uptake system and *NCX1-3*, as well as *PMCA1-4* for the plasma membrane Ca^{2+}-extrusion system, was detected in both H9 and H7 hESCs, although *SERCA1* was detected in only H9 hESCs (Figure 2D). These results indicated that hESCs express Ca^{2+} signaling regulatory machinery, including intracellular Ca^{2+} release and uptake, as well as plasma membrane Ca^{2+} influx and extrusion systems.

Ca^{2+} transients via caffeine-sensitive RyRs in a subpopulation of hESCs

To confirm whether the expressed *RyR*s are functional in these

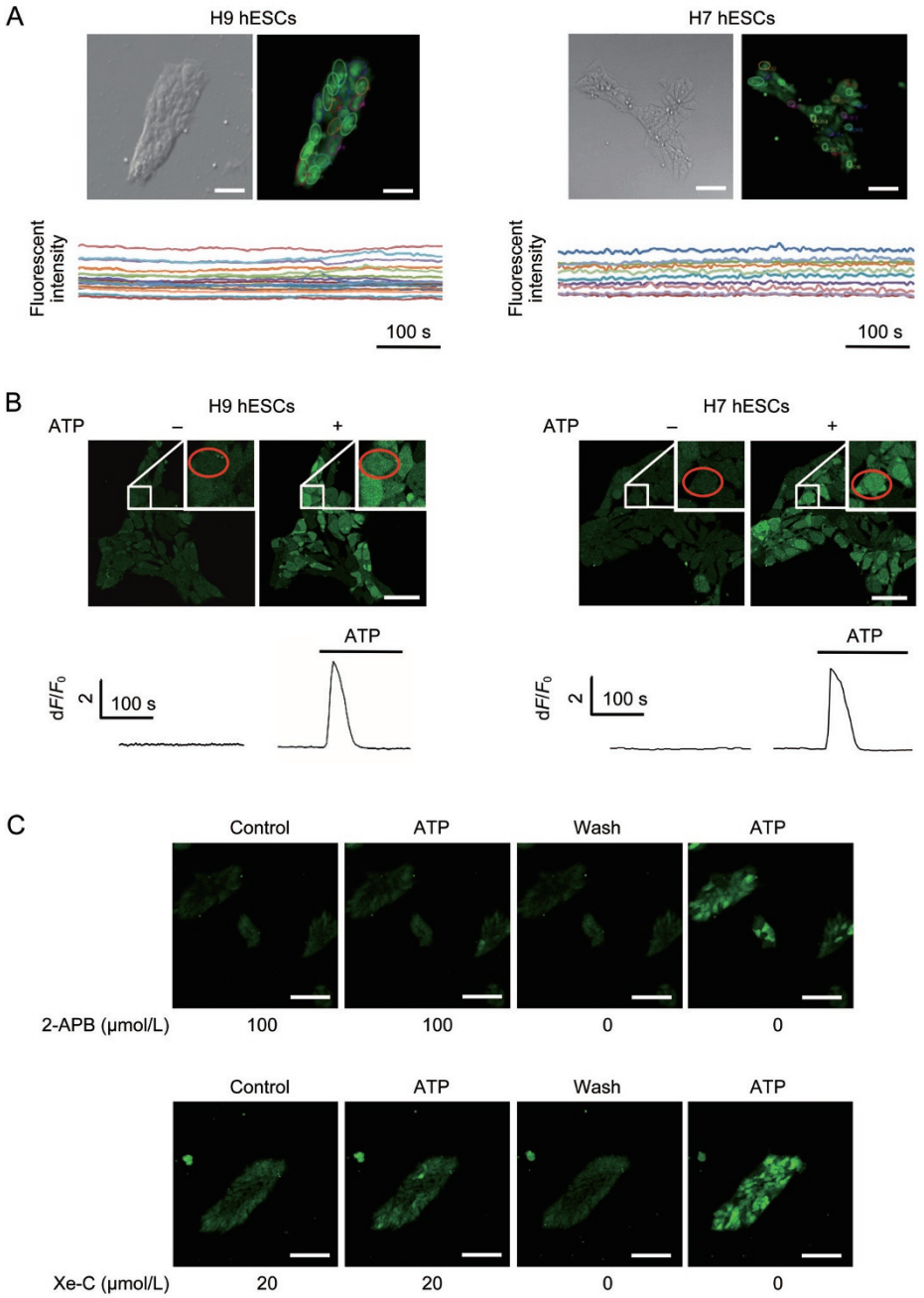

Figure 1. Spontaneous and ATP-induced Ca^{2+} activity in H9 and H7 hESCs. (A) Morphology and traces of $[Ca^{2+}]_i$. Scale bar=50 μm. (B) Representative ATP-induced (100 μmol/L) Ca^{2+} transients. Scale bar=25 μm. (C) Inhibition of ATP-induced Ca^{2+} transients by 2-APB (100 μmol/L) and xestospongin C (Xe-C, 20 μmol/L). Scale bar=50 μm. Consistent data were obtained from three to six independent experiments.

cells, we tested whether these cells respond to a RyR activator, caffeine, with release of intracellular Ca^{2+}. Caffeine at 10 mmol/L induced a rapid increase in $[Ca^{2+}]_i$ in a fraction of hESCs that responded to ATP (100 μmol/L) (Figure 3A). The amplitudes of the caffeine-induced Ca^{2+} transients were significantly lower than those induced by ATP in both H9 and H7 hESCs (Figure 3A). To determine whether the caffeine-induced increase in $[Ca^{2+}]_i$ was dependent on extracellular Ca^{2+} influx, we measured this response under Ca^{2+}-free conditions. The Ca^{2+} responses to caffeine in the Ca^{2+}-free condition were comparable to those detected in the 1.8 mmol/L Ca^{2+} solution (Figure 3B). The amplitudes of the Ca^{2+} transients (Figure 3C) and the percentages of responding cells (Figure 3D) between the 1.8 mmol/L Ca^{2+} and Ca^{2+}-free conditions were similar in both hESC lines. These data indicated that the caffeine-induced elevation of $[Ca^{2+}]_i$ is mediated by intercellular Ca^{2+} release from RyRs. This conclusion was further confirmed by the diminished caffeine-induced Ca^{2+} responses when cells were pre-incubated with a high concentration of ryanodine (10 μmol/L) (Figure 3E), which completely blocks

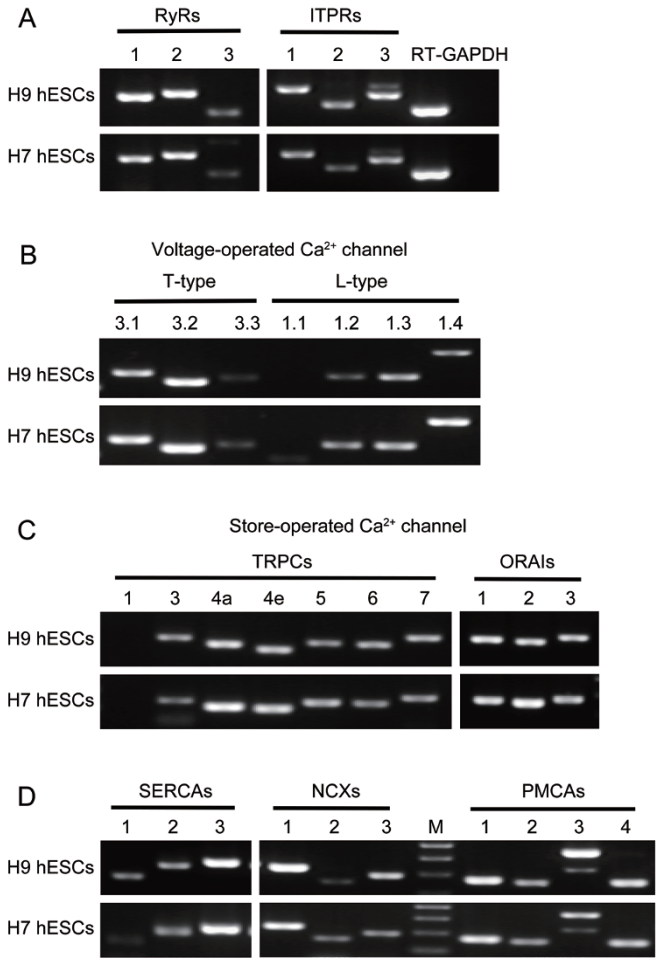

Figure 2. RT-PCR analysis of the gene expression profiles of Ca^{2+}-handling genes in H9 and H7 hESCs. (A) Gene expression of RYR1-3 and ITPR1-3. GAPDH, internal control; RT-, negative control. (B) Gene expression of voltage-operated T-type (Cav3.1–Cav3.3) and L-type (Cav1.1–Cav1.4) Ca^{2+} channels. (C) Gene expression of store-operated TPRCs and ORAIs. (D) Gene expression of SERCAs, NCXs and PMCAs. M, DNA marker. Consistent data were obtained from three independent experiments.

RyRs[22], but the high concentration of ryanodine did not affect the ATP-induced Ca^{2+} transients (Figure 3E). In addition, the amplitudes of the ATP-induced Ca^{2+} transients (Figure 3F) and percentages of Ca^{2+}-responding cells (Figure 3G) were also not affected by pretreatment with caffeine (10 mmol/L) or ryanodine (10 μmol/L) plus caffeine in these cells. Therefore, a subpopulation of H9 and H7 hESCs have functional RyRs that respond to caffeine to release Ca^{2+} from intracellular stores, but they do not contribute to the ATP-triggered Ca^{2+} transients.

Regulation of the Ca^{2+} entry system in the plasma membrane of hESCs

Next, we examined the Ca^{2+} entry pathway across the plasma membranes of hESCs. On the basis of the gene expression results, we asked whether hESCs have functional VOCCs and SOCCs. To examine this question, the cells were depolarized with a high K^+ concentration (145 mmol/L) to stimulate Ca^{2+} influx through VOCCs, as previously reported[10]. No alteration in baseline $[Ca^{2+}]_i$ was observed in both H9 and H7 hESCs (Figure 4A), thus suggesting that VOCCs are not involved in the maintenance of the baseline $[Ca^{2+}]_i$. However, this observation was not consistent with the mRNA expression of VOCC genes (*Cav3.1*, *Cav3.2*, *Cav1.2*, *Cav1.3*, *Cav1.4*) detected in hESCs (Figure 2B). We then examined the protein expression of these VOCC subtypes. Western blot analysis showed that T-type Ca^{2+} channel Cav3.2 but not Cav3.1 protein was expressed in both H7 and H9 hESCs (Figure 4B). The expression of L-type Ca^{2+} channel Cav1.2, Cav1.3 and Cav1.4 were all detected in both hESC lines (Figure 4C). Together, these results indicate that the mRNAs and proteins of T-type and L-type VOCCs are expressed in hESCs but do not appear to be functional.

To test the existence of functional SOCCs, we first incubated hESCs in Ca^{2+}-free solution to block the Ca^{2+} entry via the plasma membrane, and then applied thapsigargin (TG, 1 μmol/L), a specific SERCA inhibitor[23], to block SERCA, followed by treatment with ATP and high Ca^{2+} concentration solution as shown in Figure 4D. A transient increase in $[Ca^{2+}]_i$ was observed immediately after thapsigargin treatment in H9 and H7 hESCs (Figure 4E). Next, we applied ATP (100 μmol/L) in the Ca^{2+}-free condition to further confirm the depletion of ER Ca^{2+} stores in both cell lines (Figure 4E). Then, the bath solution was switched to a high Ca^{2+} concentration (4 mmol/L) solution, and a robust increase in $[Ca^{2+}]_i$, followed by Ca^{2+} oscillations, was observed in H9 and H7 hESCs (Figure 4E). These results indicated that SERCA is the functional ER uptake system, and SOCE but not VOCCs function as the Ca^{2+} entry pathway in hESCs.

Regulation of the Ca^{2+} extrusion system in hESCs

Because ATP- or caffeine-induced increases in $[Ca^{2+}]_i$ rapidly declined to basal levels after reaching a peak (Figure 1B and Figure 3B), the hESCs should have a robust Ca^{2+} extrusion systems and/or machinery to pump cytosolic Ca^{2+} back into the internal store. The robust increase in $[Ca^{2+}]_i$ after thapsigargin treatment (Figure 4E) indicated the involvement of functional SERCA in hESCs. PMCA and NCX are two major contributors to intracellular Ca^{2+} extrusion in most cells, including mESCs[10]. We thus examined the function of PMCA in hESCs by adding one of the most potent PMCA blockers, carboxyeosin (5 μmol/L)[24]. Carboxyeosin triggered a slow but marked increase in $[Ca^{2+}]_i$ in both H9 and H7 hESCs (Figure 5A). The amplitudes (Figure 5B) and the time to peak (Figure 5C) of Ca^{2+} transients induced by carboxyeosin were comparable in the two cell lines. Next, we examined the contribution of NCX in hESCs by application of an NCX blocker, KB-R7943[25]. KB-R7943 (100 μmol/L) induced a Ca^{2+} transient in both H9 and H7 hESCs (Figure 5D). The amplitudes (Figure 5E) and time to peak (Figure 5F) of the Ca^{2+} transients induced by KB-R7943 were comparable in the two cell lines. These data indicated that SERCA is a functional Ca^{2+} uptake machinery that works together with the PMCAs and NCXs to limit the increase of $[Ca^{2+}]_i$ and maintain a homeostatic level in hESCs.

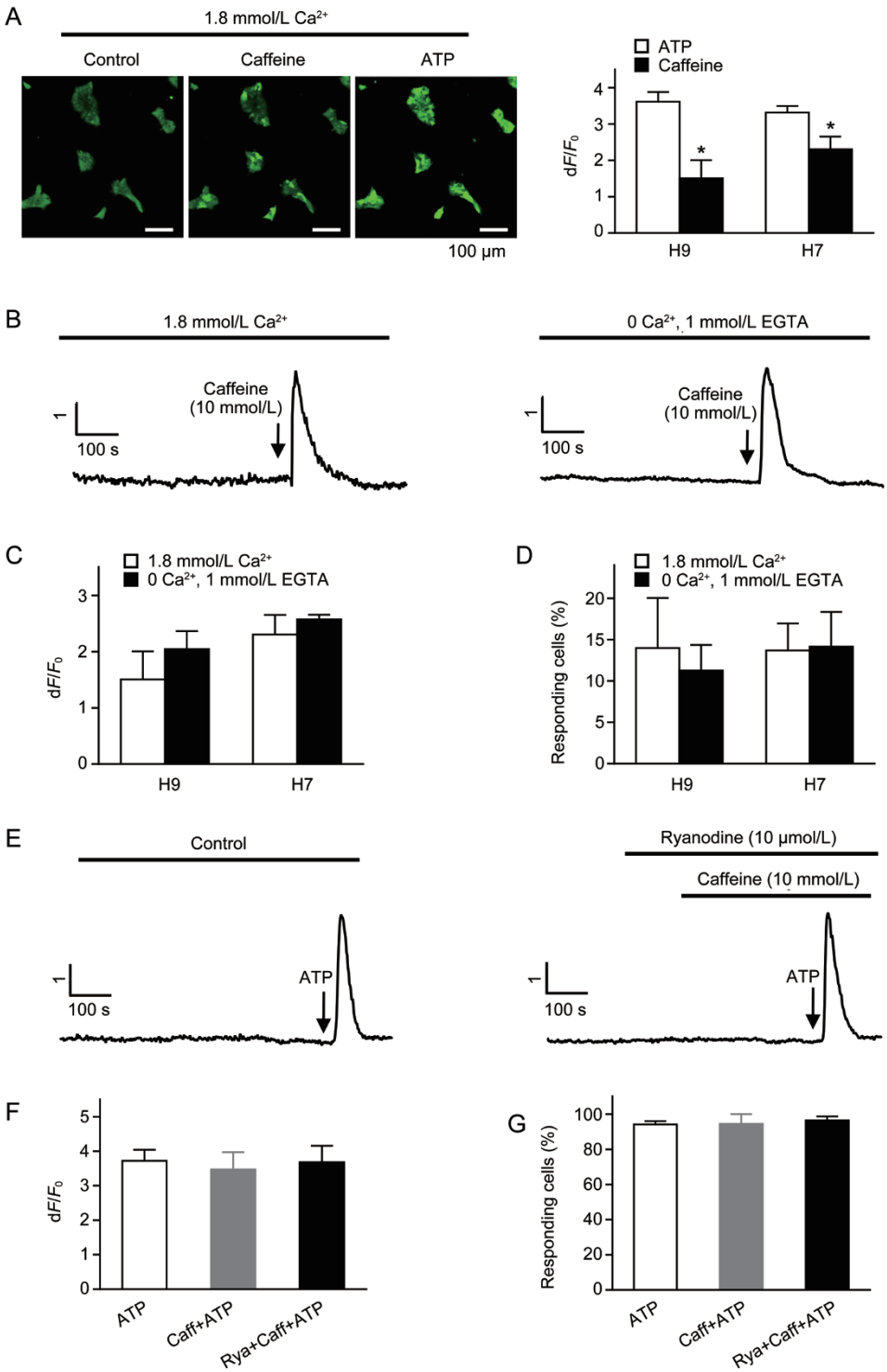

Figure 3. Ca^{2+} transients via caffeine-sensitive RyRs in a subpopulation of hESCs. (A) Ca^{2+} responses in hESCs with sequential treatment of caffeine (10 mmol/L) and ATP (100 μmol/L); representative images (left); mean amplitudes of caffeine and ATP-induced Ca^{2+} transients in H9 and H7 hESCs (right). Scale bar=100 μm. (B) Representative Ca^{2+} transients induced by caffeine (10 mmol/L) in 1.8 mmol/L Ca^{2+} (left) or Ca^{2+}-free (right) extracellular solution. (C, D) The mean amplitudes (C) and responding percentages (D) of caffeine-induced Ca^{2+} transients in 1.8 mmol/L Ca^{2+} or Ca^{2+}-free extracellular solution. (E) Representative trace of ATP-induced (100 μmol/L) Ca^{2+} transient in the control (left) or ryanodine+caffeine pre-incubated condition (right). (F, G) The mean amplitudes (F) and responding percentages (G) of ATP-responding cells in the control (ATP), caffeine (Caff+ATP) or ryanodine+caffeine (Rya+Caff+ATP) pre-incubated condition. *n*=3, 30–50 hESCs in each experiment.

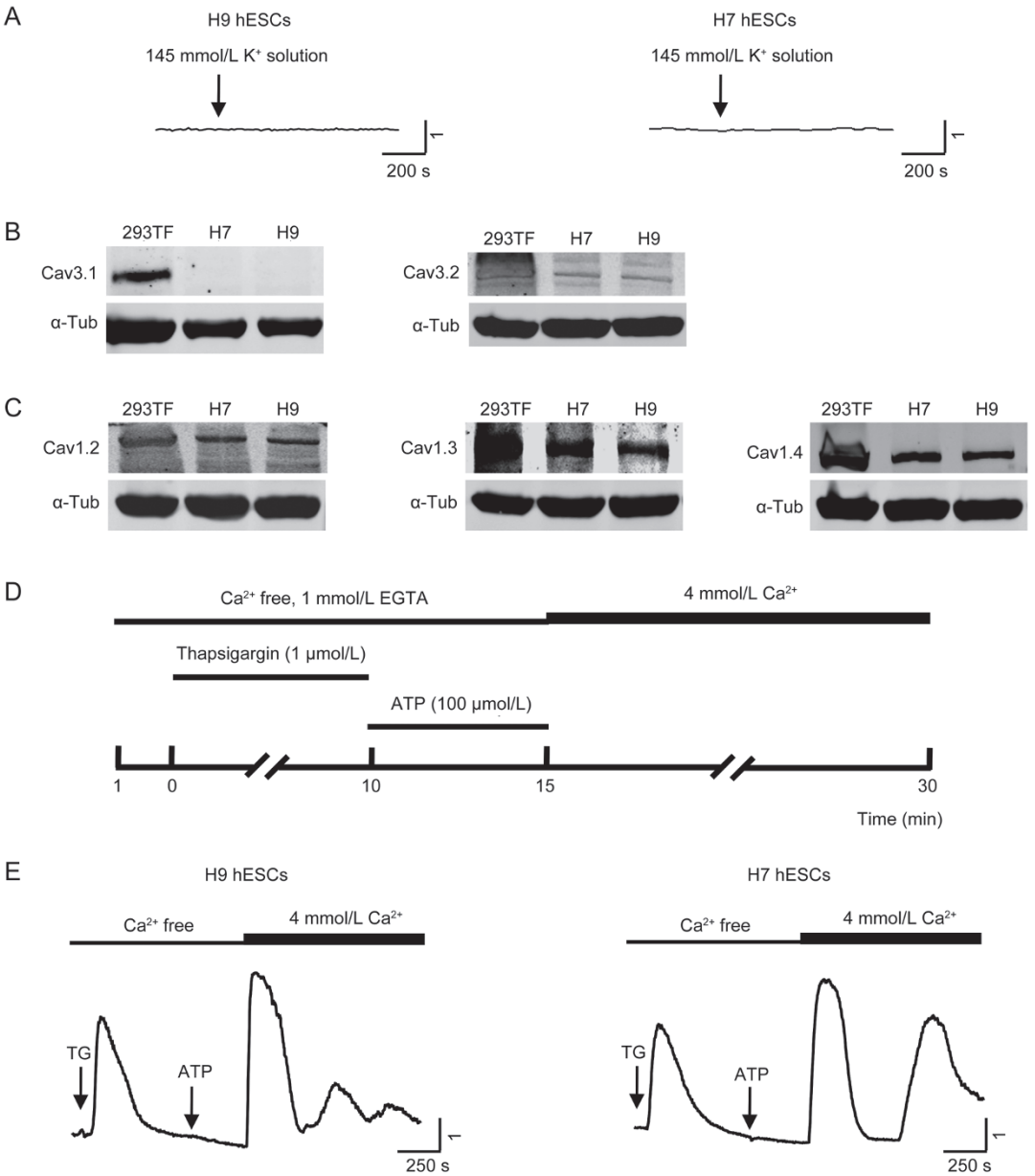

Figure 4. Ca^{2+} entry machinery of the plasma membrane and the protein expression of VOCCs in H9 and H7 hESCs. (A) $[Ca^{2+}]_i$ recording in hESCs with a high K^+ concentration (145 mmol/L) in the extracellular solution. (B) Western blot analysis of T-type Ca^{2+} channels Cav3.1 and Cav3.2 in H7 and H9 cells. 293FT was used as a positive control. Data shown are representative of three independent experiments. (C) Western blot analysis of L-type Ca^{2+} channels Cav1.2, Cav1.3 and Cav1.4 in H7 and H9 cells. 293FT was used as a positive control. Data shown are representative of three independent experiments. α-Tub, α-tubulin, an internal control. (D) An outline of the experimental protocol for measuring SOCE. (E) Representative traces of Ca^{2+} signals in hESCs with the various treatments as shown in (D). TG, thapsigargin (1 μmol/L); ATP, 100 μmol/L. Consistent data were obtained from three independent experiments and 50 hESCs in each experiment from each cell line.

Discussion

The main findings of the present study are that (i) hESCs do not have spontaneous Ca^{2+} transients in the steady state; (ii) IP_3R-mediated Ca^{2+} release is a major source of $[Ca^{2+}]_i$ elevation during the G-protein-coupled receptor (GPCR) activation, whereas functional RyRs exist in a subpopulation of hESCs; (iii) Ca^{2+} entry through the store-operated Ca^{2+} channels participates in the maintenance of the steady state of $[Ca^{2+}]_i$ in hESCs; and (iv) SERCA is the main machinery pumping cytosolic Ca^{2+} back into the internal store and works together with the Ca^{2+} extrusion machinery of PMCA and NCX to transport Ca^{2+} out of the cell, thus resulting in a decrease in $[Ca^{2+}]_i$. These findings provide new insights into the physiological and pharmacological properties of hESCs by revealing the Ca^{2+} signaling regulatory mechanisms.

Here, we investigated the Ca^{2+} signal properties in hESCs

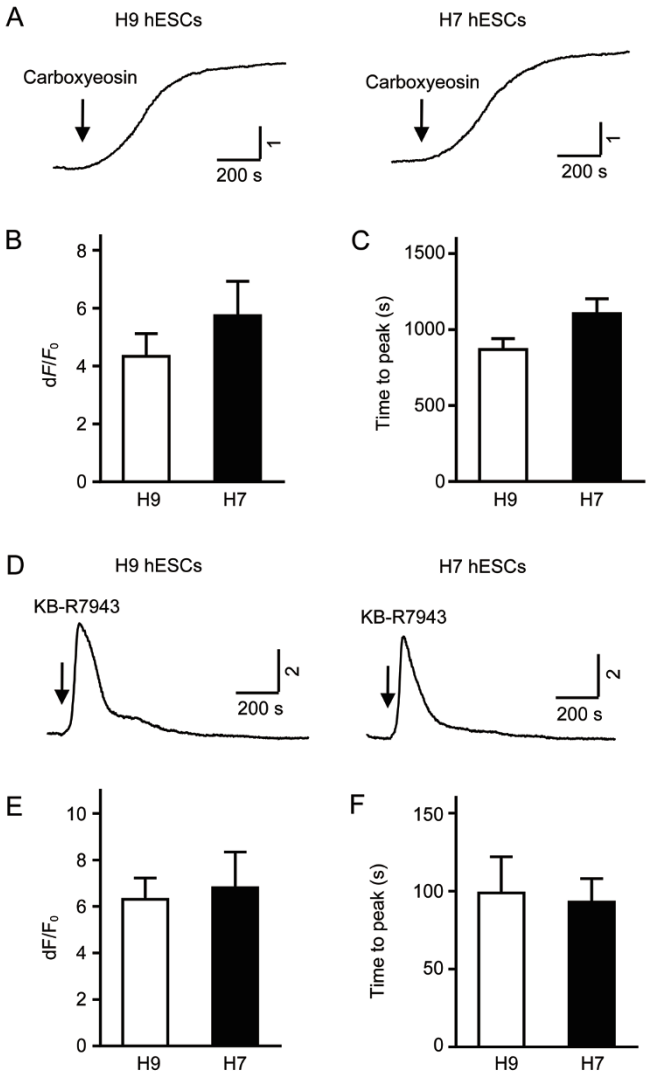

Figure 5. Regulation of Ca^{2+} extrusion in H9 and H7 hESCs. (A) $[Ca^{2+}]_i$ recording in hESCs in the presence of a PMCA inhibitor, carboxyeosin (5 μmol/L). (B, C) The mean amplitudes (B) and time to peak (C) of the carboxyeosin-induced $[Ca^{2+}]_i$ elevation. (D) Representative traces of Ca^{2+} transients induced by an NCX inhibitor, KB-R7943 (100 μmol/L). (E, F) The mean amplitudes (E) and time to peak (F) of KB-R7943-induced Ca^{2+} transients. Data were collected from three independent experiments and 40–50 hESCs in each experiment from each cell line.

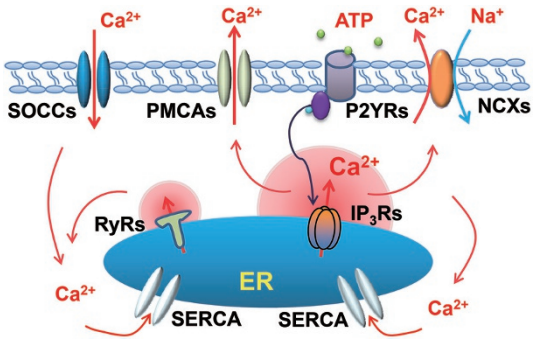

Figure 6. A working model for Ca^{2+} signaling regulatory machinery in hESCs.

both in basal and activated conditions. In contrast to the active Ca^{2+} transients in mESCs[12], the level of $[Ca^{2+}]_i$ is stable in steady-state hESCs, thus indicating that Ca^{2+} homeostasis is a hallmark of hESCs. In contrast, a GPCR agonist such as ATP triggers a rapid and robust increase in $[Ca^{2+}]_i$ via IP_3R-mediated intracellular Ca^{2+} release in hESCs. However, the IP_3R-mediated Ca^{2+} signals do not appear to be the only available intracellular Ca^{2+} sources in hESCs because approximately 10%–15% of cells of both hESC lines respond to both ATP and caffeine stimulation, and the expression of type 1 and type 2 RyRs is detected, thus suggesting the existence of a subpopulation of hESCs expressing both IP_3Rs and RyRs. This phenomenon is controversial in mESCs, because Yanagida *et al* have reported that the mESC line ES-D3 does not respond to caffeine at all[10], whereas Mamo *et al* have reported that the response to caffeine is cell line-dependent in mESCs[26]. The current data suggest that hESCs might be divided into subpopulations with heterogenic regulation of the intracellular Ca^{2+} release system. However, we found that in the Ca^{2+} response to caffeine, the function of this Ca^{2+} release machinery, most probably RyRs, might be immature, because the mean amplitude of the Ca^{2+} transients induced by caffeine was much lower than that induced by ATP (Figure 3A). Subcloning these populations of hESCs would be useful for investigating the physiological relevance of the caffeine-responding hESC subpopulation to the self-renewal and differentiation capacity.

There are a number of channels that might be responsible for the Ca^{2+} entry on the plasma membrane. VOCCs comprise a large family of Ca^{2+} channels that function primarily in electrically excitable cells, such as neurons and muscle cells. In this study, we focused on the non-neuronal L-type and T-type VOCCs. However, these VOCCs did not function well in hESCs. Although both the mRNA and protein of Cav3.2 (T-type), Cav1.2, Cav1.3 and Cav1.4 (L-type) Ca^{2+} channels are expressed in H9 and H7 hESCs, depolarization of the membrane potential by a high K^+ solution did not trigger $[Ca^{2+}]_i$ changes (Figure 4A). This result was consistent with previous studies reporting that depolarization-induced Ca^{2+} entry was not observed in ES-D3 mESCs[10], H1 hESCs[27] or CCTL-14 hESCs[28] after stimulation by either a high K^+ extracellular solution or depolarized during patch-clamp analysis, though a Ca^{2+} current via Cav3.2 has been detected in an independent study in 46.7% of R1 mESCs[27]. Together with these previous observations, our results suggest that hESCs might be voltage-insensitive cells, and the VOCCs in hESCs might require additional regulatory mechanisms, such as to work in combination with other subunits or protein modifications[29], to function in modulating Ca^{2+} signals during differentiation. SOCCs are the Ca^{2+} channels responsible for the concept of store-operated Ca^{2+} entry. TPRC and ORAI channels are two types of well documented SOCCs[30–32]. In agreement with the observations from mESCs[10], hESCs express functional SOCCs

(Figure 4E). Our data indicated that the Ca^{2+} entry via the plasma membrane is mainly from SOCCs but not VOCCs in hESCs. In addition, we have recently demonstrated that ATP-activated P2X receptors (a type of ligand-gated Ca^{2+} channels) have only a small contribution to ATP-induced Ca^{2+} responses in hESCs[5]. In contrast, ATP-induced Ca^{2+} transients were completely inhibited by IP_3R blockers (Figure 1C). Thus, Ca^{2+} entry through the plasma membrane is not a major source of ATP-induced Ca^{2+} transients but might act as a re-filling mechanism. Because hESCs did not show active spontaneous Ca^{2+} activity (Figure 1A), the ER Ca^{2+} store was not depleted during the steady state; thus, determining the physiological relevance of SOCE during the differentiation of hESCs is of interest.

Furthermore, we detected functional SERCA, NCX and PMCA in hESCs, a result is consistent with the Ca^{2+} uptake and extrusion pathway in mESCs[10]. In addition, a comparable role of these pathways was observed in both hESC cell lines (Figure 5B, 5C and 5D–5F), thus indicating the conserved role of this Ca^{2+} regulatory machinery between different hESC cell lines. The thapsigargin-induced increase in $[Ca^{2+}]_i$ indicated that hESCs have functional SERCAs and ER Ca^{2+} leak. Given that no spontaneous Ca^{2+} activity is detected in hESCs, one possibility for this phenomenon is that the ER Ca^{2+} leak (from channels such as IP_3Rs and RyRs) reaches a steady-state balance with the Ca^{2+} pumped back through SERCA. Another possibility is that the Ca^{2+} leak might not reach a threshold to initiate a spontaneous increase in $[Ca^{2+}]_i$. The spontaneous increase in $[Ca^{2+}]_i$ is a 'big Ca^{2+} event' inside of a cell that requires the opening of Ca^{2+} channels to reach a threshold[33]. In other words, even with the opening of a single active Ca^{2+} channel (such as Ca^{2+} leak through a single IP_3R or RyR), there might not be any Ca^{2+} events, such as Ca^{2+} puffs or sparks, as well as global Ca^{2+} activity, such as Ca^{2+} transients or waves[34], formed by groups of channels unless the initial event reaches the threshold. Further studies using methods such as line-scan confocal imaging in hESCs are needed to address this issue.

Notably, different patterns in the trace of $[Ca^{2+}]_i$ elevation induced by thapsigargin, carboxyeosin and KB-R7943 were observed (Figure 4E, 5A and 5D). These results may be explained at least partially by the differential Ca^{2+} regulators involved and distinct Ca^{2+} mobilizing kinetics of these channels: (i) the fast decay of $[Ca^{2+}]_i$ in the thapsigargin-induced Ca^{2+} transient may have resulted from the depletion of the ER Ca^{2+} store and the activation of PMCA and/or NCX; (ii) the fast decay of $[Ca^{2+}]_i$ in the KB-R7943-induced Ca^{2+} transient may have resulted from the Ca^{2+} uptake through SERCA and its extrusion by PMCA; and (iii) the continuous elevation of $[Ca^{2+}]_i$ induced by carboxyeosin may have resulted from the less functional NCX because of the slow change in $[Ca^{2+}]_i$ induced by carboxyeosin, which is not considered optimal for NXC functioning[35]. NCX is a Ca^{2+} exchanger with low Ca^{2+} affinity and high capacity, whereas PMCA has a high Ca^{2+} affinity but low capacity and fine-tunes cytosolic $[Ca^{2+}]_i$ because it can function in the concentration range in which NCX is relatively inefficient[36]. In addition, NCX and PMCA have different roles in the extrusion of Ca^{2+} out of cells during SOCE or capacitative Ca^{2+} entry, and the decay in $[Ca^{2+}]_i$ from the peak to baseline is mainly due to Ca^{2+} removal via PMCA[35]. Therefore, inhibition of SERCA or NCX leads to an increase in $[Ca^{2+}]_i$ and then a quick decrease to baseline, whereas inhibition of PMCA leads to a sustained increase in $[Ca^{2+}]_i$.

These results, together with our previous findings of the functional response of IP_3Rs to purinergic stimulation[5], indicated that hESCs already have a functional ER, which serves as a powerful regulator controlling homeostasis of $[Ca^{2+}]_i$ through Ca^{2+}-release channels, such as IP_3Rs and RyRs, and Ca^{2+} pumps, such as SERCA, and works together with receptors, pumps and exchangers in the plasma membrane.

In conclusion, the present study established a working model of Ca^{2+} signaling regulatory machinery in hESCs (Figure 6): ATP-elevated $[Ca^{2+}]_i$ is mediated primarily by Ca^{2+} release from intracellular stores through IP_3Rs. Moreover, intracellular Ca^{2+} release can be induced by caffeine-sensitive RyRs in a subpopulation of hESCs, thus indicating the heterogeneity of Ca^{2+} signaling machinery in hESCs. In addition, the refilling of the intracellular Ca^{2+} store is mediated by SOCE of hESCs. The low level of $[Ca^{2+}]_i$ is maintained by uptake of cytosolic free Ca^{2+} back to intracellular stores through SERCA and Ca^{2+} extrusion via NCXs and PMCAs. These data reveal previously unrecognized Ca^{2+} signaling regulatory pathways in the maintenance of Ca^{2+} homeostasis in hESCs.

Acknowledgements

This work was supported by grants from the National Natural Science of China (No 81520108004, 81470422 and 31030050 to HTY, No 31401167 to MZ), the National Basic Research Program of China (No 2014CB965100 to Huang-tian YANG), the National Science and Technology Major Project (No 2012ZX09501001 to Huang-tian YANG), the National Key Research and Development Program (2016YFC1301200 to Huang-tian YANG), and the Natural Science Foundation of Shanghai (No 17ZR1435500 to Jin-jun HUANG).

We thank WiCell Research Institute for providing the H7 and H9 hESCs and Dr He-ping CHENG (Peking University, Beijing, China) for providing the Flash Sniper software.

Author contribution

Ji-jun HUANG, Yi-jie WANG, and Min ZHANG contributed to the study conception and design, collection of data, data analysis, interpretation and manuscript writing; Peng ZHANG contributed to the Ca^{2+} imaging experiments, western blot experiments and hESC culture; He LIANG and Hua-jun BAI contributed to the hESC culture; Xiu-jian YU provided experimental assistance and contributed to the data analysis; Huang-tian YANG contributed to the conception and design of the experiments, data analysis and interpretation, manuscript writing, financial support and final approval of the manuscript.

Supplementary information

Supplementary information is available at the website of Acta

Pharmacologica Sinica.

References

1 Bellamy V, Vanneaux V, Bel A, Nemetalla H, Emmanuelle Boitard S, Farouz Y, *et al.* Long-term functional benefits of human embryonic stem cell-derived cardiac progenitors embedded into a fibrin scaffold. J Heart Lung Transplant 2015; 34: 1198–207.

2 Menasche P, Vanneaux V, Hagege A, Bel A, Cholley B, Cacciapuoti I, *et al.* Human embryonic stem cell-derived cardiac progenitors for severe heart failure treatment: first clinical case report. Eur Heart J 2015; 36: 2011–7.

3 Passier R, van Laake LW, Mummery CL. Stem-cell-based therapy and lessons from the heart. Nature 2008; 453: 322–9.

4 Blin G, Nury D, Stefanovic S, Neri T, Guillevic O, Brinon B, *et al.* A purified population of multipotent cardiovascular progenitors derived from primate pluripotent stem cells engrafts in postmyocardial infarcted nonhuman primates. J Clin Invest 2010; 120: 1125–39.

5 Huang J, Zhang M, Zhang P, Liang H, Ouyang K, Yang HT. Coupling switch of P2Y-IP3 receptors mediates differential Ca^{2+} signaling in human embryonic stem cells and derived cardiovascular progenitor cells. Purinergic Signal 2016; 12: 465–78.

6 Apati A, Berecz T, Sarkadi B. Calcium signaling in human pluripotent stem cells. Cell Calcium 2016; 59: 117–23.

7 Apati A, Paszty K, Hegedus L, Kolacsek O, Orban TI, Erdei Z, *et al.* Characterization of calcium signals in human embryonic stem cells and in their differentiated offspring by a stably integrated calcium indicator protein. Cell Signal 2013; 25: 752–9.

8 Ermakov A, Pells S, Freile P, Ganeva VV, Wildenhain J, Bradley M, *et al.* A role for intracellular calcium downstream of G-protein signaling in undifferentiated human embryonic stem cell culture. Stem Cell Res 2012; 9: 171–84.

9 Apati A, Paszty K, Erdei Z, Szebenyi K, Homolya L, Sarkadi B. Calcium signaling in pluripotent stem cells. Mol Cell Endocrinol 2012; 353: 57–67.

10 Yanagida E, Shoji S, Hirayama Y, Yoshikawa F, Otsu K, Uematsu H, *et al.* Functional expression of Ca^{2+} signaling pathways in mouse embryonic stem cells. Cell Calcium 2004; 36: 135–46.

11 Tonelli FM, Santos AK, Gomes DA, da Silva SL, Gomes KN, Ladeira LO, *et al.* Stem cells and calcium signaling. Adv Exp Med Biol 2012; 740: 891–916.

12 Kapur N, Mignery GA, Banach K. Cell cycle-dependent calcium oscillations in mouse embryonic stem cells. Am J Physiol Cell Physiol 2007; 292: C1510–8.

13 Cao N, Liang H, Huang J, Wang J, Chen Y, Chen Z, *et al*. Highly efficient induction and long-term maintenance of multipotent cardiovascular progenitors from human pluripotent stem cells under defined conditions. Cell Res 2013; 23: 1119–32.

14 Li K, Zhang W, Liu J, Wang W, Xie W, Fang H, *et al*. Flash sniper: automated detection and analysis of mitochondrial superoxide flash. Biophys J 2009; 96: 531a–32a.

15 Mikoshiba K. IP_3 receptor/Ca^{2+} channel: from discovery to new signaling concepts. J Neurochem 2007; 102: 1426–46.

16 Gafni J, Munsch JA, Lam TH, Catlin MC, Costa LG, Molinski TF, *et al.* Xestospongins: potent membrane permeable blockers of the inositol 1,4,5-trisphosphate receptor. Neuron 1997; 19 : 723–33.

17 Lanner JT, Georgiou DK, Joshi AD, Hamilton SL. Ryanodine receptors: structure, expression, molecular details, and function in calcium release. Cold Spring Harb Perspect Biol 2010; 2: a003996.

18 Rossier MF. T-type calcium channel: a privileged gate for calcium entry and control of adrenal steroidogenesis. Front Endocrinol 2016; 7: 43.

19 Dolphin AC. L-type calcium channel modulation. Adv Second Messenger Phosphoprotein Res 1999; 33: 153–77.

20 Ong HL, de Souza LB, Ambudkar IS. Role of TRPC channels in store-operated calcium entry. Adv Exp Med Biol 2016; 898: 87–109.

21 Sabourin J, Bartoli F, Antigny F, Gomez AM, Benitah JP. Transient receptor potential canonical (TRPC)/Orai1-dependent store-operated Ca^{2+} channels: new targets of aldosterone in cardiomyocytes. J Biol Chem 2016; 291: 13394–409.

22 Yang HT, Tweedie D, Wang S, Guia A, Vinogradova T, Bogdanov K, *et al.* The ryanodine receptor modulates the spontaneous beating rate of cardiomyocytes during development. Proc Natl Acad Sci U S A 2002; 99: 9225–30.

23 Michelangeli F, East JM. A diversity of SERCA Ca^{2+} pump inhibitors. Biochem Soc Trans 2011; 39: 789–97.

24 Green AK, Cobbold PH, Dixon CJ. Effects on the hepatocyte $[Ca^{2+}]i$ oscillator of inhibition of the plasma membrane Ca^{2+} pump by carboxyeosin or glucagon-(19–29). Cell Calcium 1997; 22: 99–109.

25 Sibarov DA, Abushik PA, Poguzhelskaya EE, Bolshakov KV, Antonov SM. Inhibition of plasma membrane Na/Ca-exchanger by KB-R7943 or lithium reveals its role in Ca-dependent *N*-methyl-*D*-aspartate receptor Inactivation. J Pharmacol Exp Ther 2015; 355: 484–95.

26 Mamo S, Kobolak J, Borbiro I, Biro T, Bock I, Dinnyes A. Gene targeting and calcium handling efficiencies in mouse embryonic stem cell lines. World J Stem Cells 2010; 2: 127-40.

27 Rodriguez-Gomez JA, Levitsky KL, Lopez-Barneo J. T-type Ca^{2+} channels in mouse embryonic stem cells: modulation during cell cycle and contribution to self-renewal. Am J Physiol Cell Physiol 2012; 302: C494–504.

28 Forostyak O, Romanyuk N, Verkhratsky A, Sykova E, Dayanithi G. Plasticity of calcium signaling cascades in human embryonic stem cell-derived neural precursors. Stem Cells Dev 2013; 22: 1506–21.

29 Catterall WA, Swanson TM. Structural basis for pharmacology of voltage-gated sodium and calcium channels. Mol Pharmacol 2015; 88: 141–50.

30 Hogan PG, Rao A. Store-operated calcium entry: mechanisms and modulation. Biochem Biophys Res Commun 2015; 460: 40–9.

31 Albarran L, Lopez JJ, Salido GM, Rosado JA. Historical overview of store-operated Ca^{2+} entry. Adv Exp Med Biol 2016; 898: 3–24.

32 Lopez JJ, Albarran L, Gomez LJ, Smani T, Salido GM, Rosado JA. Molecular modulators of store-operated calcium entry. Biochim Biophys Acta 2016; 1863: 2037–43.

33 Foskett JK, White C, Cheung KH, Mak DO. Inositol trisphosphate receptor Ca^{2+} release channels. Phys Rev 2007; 87: 593–658.

34 Berridge MJ, Lipp P, Bootman MD. The versatility and universality of calcium signalling. Nat Rev Mol Cell Biol 2000; 1: 11–21.

35 Klishin A, Sedova M, Blatter LA. Time-dependent modulation of capacitative Ca^{2+} entry signals by plasma membrane Ca^{2+} pump in endothelium. Am J Physiol 1998; 274: C1117–28.

36 Brini M, Carafoli E. The plasma membrane Ca^{2+} ATPase and the plasma membrane sodium calcium exchanger cooperate in the regulation of cell calcium. Cold Spring Harb Perspect Biol 2011; 3. Doi: 10.1101/cshperspect.a004168.